CROATICA CHEMICA ACTA
CCACAA **81** (4) 569–578 (2008)
ISSN-0011-1643
CCA-3276
Original Scientific Paper

Investigation of Factors Influencing the Precipitation of Iron Oxides from Fe(II) Containing Solutions

Marijan Gotić[a,*], Svetozar Musić[a,*], Stanko Popović[b], and Lavoslav Sekovanić[c]

[a]*Division of Materials Chemistry, Ruđer Bošković Institute, P. O. Box 180, HR-10002, Zagreb, Croatia*

[b]*Department of Physics, Faculty of Natural Sciences and Mathematics, University of Zagreb, P. O. Box 331, HR-10002 Zagreb, Croatia*

[c]*Faculty of Geotechnical Engineering, University of Zagreb, Hallerova 7, HR-42000, Varaždin, Croatia*

RECEIVED SEPTEMBER 24, 2007; REVISED NOVEMBER 28, 2007; ACCEPTED DECEMBER 10, 2007

Factors that influence the precipitation of iron oxides from Fe(II) containing solutions were investigated by X-ray powder diffraction, ^{57}Fe Mössbauer and FT-IR spectroscopies, FE SEM and EDS techniques. Near spherical aggregates of spindle-shape goethite particles were obtained by oxidation of 0.1 mol dm^{-3} $FeSO_4$ solution (suspension) with pure oxygen at 90 °C. Wide and thin goethite particles elongated along the crystallographic *c*-axis were formed in parallel. With the addition of tetramethylammonium hydroxide to 0.1 mol dm^{-3} $FeSO_4$ solution (suspension) substoichiometric magnetite ($Fe_{3-x}O_4$) particles were additionally formed. They were dominant at pH > 12.5. Mössbauer spectroscopy was used to calculate the stoichiometries of $Fe_{3-x}O_4$ particles. Very small magnetite particles (≈ 20–100 nm) showed a tendency to aggregate. The twinning effect of octahedral magnetite particles (> 200 nm) was observed. A drastic effect on the properties of iron oxide precipitates was achieved by adding H_3PO_4 to the precipitation system containing 0.1 mol dm^{-3} $FeSO_4$ + 0.01 mol dm^{-3} H_2SO_4 solution at the start. In dependence on the concentration of the added H_3PO_4, nanosize goethite particles about 15–25 nm in size, or poor crystalline ferrihydrite particles (two-line ferrihydrite) were obtained. The EDS analyses of the precipitates did not show any significant change in the sulphur content, whereas the phosphorous content gradually increased in the precipitates with an increase in the added H_3PO_4. In high concentrations phosphates completely suppressed the formation of goethite under given experimental conditions, and phosphated ferrihydrite was formed instead.

Keywords
ferrihydrite
magnetite
phosphate
Mössbauer
FE SEM

INTRODUCTION

Synthetic iron oxides have found various applications in industry, as pigments, catalysts, magnetic inks, sensors, materials against unwanted electromagnetic radiation, as raw materials in the synthesis of ferrites, *etc*. Recently, maghemite (γ-Fe_2O_3) and magnetite (Fe_3O_4) have found important applications in biomedicine.

At the laboratory level, iron oxides can be prepared using different procedures, such as slow or forced hydrolysis of iron(III)-salts, crystallization from dense ferrihydrite gel, oxidation of $Fe(OH)_2$ gel or thermal decomposition of various iron-organic compounds.[1] Very small iron oxide particles can be produced by aerosol pyrolysis, sol-gel and microemulsion methods. Phase composition,

* Authors to whom correspondence should be addressed. (E-mail: music@irb.hr; gotic@irb.hr)

TABLE I. Experimental conditions for the preparation of samples at 90 °C and crystalline phases as found by X-ray powder diffraction

Sample	$V(H_2O)$ / mL	V(TMAH[(b)]) / mL	V(0.5 mol dm^{-3} H_3PO_4) / mL	$c(FeSO_4)$ / mol dm^{-3}	Type of bubbling	Final pH (approx.)	Crystalline phases
S1	200			0.1	O_2	1.7	G
S2	195	5		0.1	O_2	5.0	G + M
S3	180	20		0.1	O_2	12.5	M + G
S4	160	40		0.1	O_2	>13	M + G
S5	195[(a)]	5		0.1	O_2	5.0	G + M
S6	193[(a)]	5	2	0.1	O_2	4.5	G
S7	190[(a)]	5	5	0.1	O_2	4.5	FH
S8	185[(a)]	5	10	0.1	O_2	4.0	FH + X

[(a)] 0.01 mol dm^{-3} H_2SO_4 aqueous solution was used
[(b)] tetramethylammonium hydroxide (w = 25 %)
G = goethite
M = magnetite
FH = two-line ferrihydrite
X = unidentified peaks

size, geometrical shape and other properties of iron oxide particles depend on the specific synthesis method and the nature of the chemical precursor used. For this reason, many researchers are investigating factors that influence the precipitation of iron oxides and their properties.

The presence of various anions in the precipitation systems is also manifested by a strong effect on the formation of iron oxides in aqueous media. This is specifically related to the precipitation systems containing sulphate anions. In the case of $FeSO_4$ solutions, oxidation of Fe^{2+} ions occurs, which has an additional influence on the phase composition and other properties of the iron oxide precipitates formed. Musić *et al.*[2–5] investigated the precipitation of iron oxides from $FeSO_4$ solutions and the effect of various experimental factors on the phase composition of the corresponding precipitates. The phase composition of the precipitates strongly depended on the $[Fe^{2+}]/[OH^-]$ concentration ratio at the beginning of the precipitation process, the rate of Fe^{2+} oxidation, precipitation time, temperature and the kind of alkali added as a precipitating agent. The presence of sulphate anions also strongly influences the precipitation processes of Fe^{3+} ions in aqueous media. For example, forced hydrolyses of Fe^{3+} ions in the presence of sulphate anions yielded basic iron(III)-sulphates.[6–9] The $FeSO_4^+$ complex suppressed hydroxy polymerization and formation of oxyhydroxides and oxides. Basic iron(III)-sulphates were formed instead.

In the present investigation we have focused on some additional factors influencing the precipitation of iron oxides from $FeSO_4$ solutions. Tetramethylammonium hydroxide (TMAH) as a strong organic alkali was used as the precipitating agent, instead of NaOH or KOH. The effects of TMAH and H_3PO_4 addition to the phase composition of iron oxide precipitates as well as the size and morphology of the particles in the precipitates were investigated with the aim to obtain additional data about these precipitation systems.

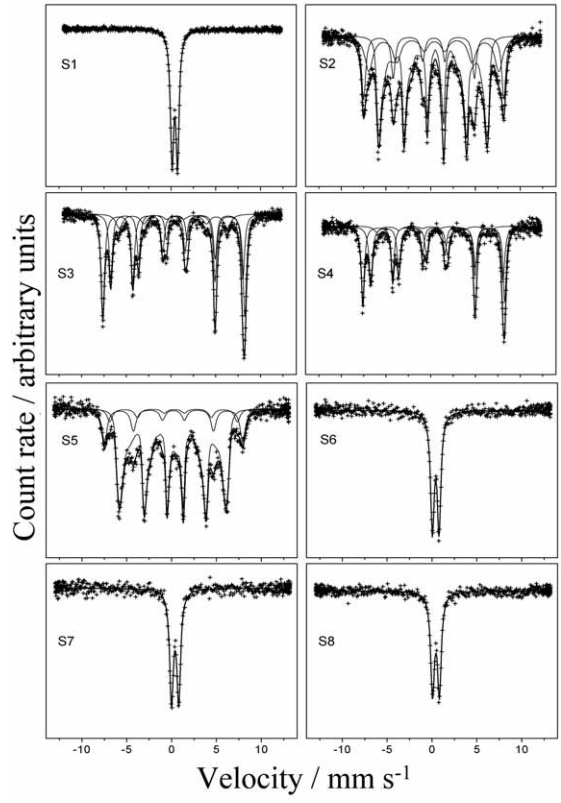

Figure 1. ^{57}Fe Mössbauer spectra of samples S1 to S8, recorded at 20 °C.

EXPERIMENTAL

The chemicals, H_3PO_4, H_2SO_4 and $FeSO_4 \cdot 7H_2O$, were of analytical purity. The oxidation state of Fe^{2+} ions in the $FeSO_4 \cdot 7H_2O$ salt was confirmed by Mössbauer spectroscopy. Aqueous solution of TMAH (mass fraction, w = 25 %) and electronic grade (99.999 %) was supplied by *Alfa Aesar*®. Twice-distilled water was used. Precipitation was done in the round-bottom boiling glass flask with four inlet

TABLE II. ^{57}Fe Mössbauer parameters calculated for samples S1 to S8 and identification of crystal phases

Sample	Fitting procedure	δ / mm s^{-1}	Δ or E_q / mm s^{-1}	B_{hf} / T	Γ / mm s^{-1}	Area / %	Phase composition	Phase fraction
S1	Q	0.41	0.61		0.44	100	Superparamagnetic particles[(a)]	1.00
S2	M1	0.33	–0.01	48.56	0.56	22.4	Substoichiometric magnetite ($Fe_{2.89}O_4$)	0.41
	M2	0.37	–0.07	44.82	0.97	19.0		
	G2	0.37	–0.27	31.88	0.30	58.6	Goethite	0.59
S3	M1	0.31	–0.01	49.19	0.45	50.8	Substoichiometric magnetite ($Fe_{2.86}O_4$)	0.86
	M2	0.64	–0.00	45.83	0.45	34.7		
	G1	0.33	–0.17	37.53	0.97	14.5	Goethite	0.14
S4	M1	0.33	–0.01	49.17	0.41	47.8	Substoichiometric magnetite ($Fe_{2.90}O_4$)	0.93
	M2	0.68	–0.02	45.85	0.49	45.4		
	G1	0.16	0.19	39.07	0.77	6.8	Goethite	0.07
S5	G1	0.26	–0.26	29.81	0.29	77.5	Goethite	0.78
	M1	0.21	0.02	47.81	0.71	15.9	Substoichiometric magnetite ($Fe_{2.80}O_4$)	0.22
	M2	0.26	–0.09	44.13	0.73	6.5		
S6	Q	0.41	0.74		0.49	100	Ferrihydrite[(a)]	1.00
S7	Q	0.38	0.81		0.50	100	Ferrihydrite[(a)]	1.00
S8	Q	0.43	0.76		0.51	100	Ferrihydrite[(a)]	1.00

Key: δ = isomer shift given relative to α-Fe at RT, E_q = quadrupole splitting, B_{hf} = hyperfine magnetic field, Γ = line width
Error: δ = ± 0.01 mm s^{-1}, E_q = ± 0.01 mm s^{-1}, B_{hf} = ± 0.2 T
Notes: Q = paramagnetic doublet; G1 = goethite patterns fitted to the distribution of hyperfine magnetic fields; G2 = goethite patterns fitted without a distribution of hyperfine magnetic fields; M1 = outer sextet of magnetite; M2 = inner sextet of magnetite
[(a)] Crystalline phases were determined considering also the results of XRD measurements

necks. A water-cooled reflux condenser was mounted onto the reaction vessel. A glass stirrer was rotated by a small electromotor and the angular speed of the stirrer was measured. The reaction vessel was isolated from the glass mixer by a specially designed adapter filled with silicon oil. A pure O_2 or N_2 gas was cleaned with a series of in-line filters between gas cylinders and the reaction vessel. After 6 h of precipitation the chemical reactions were stopped and the precipitates were separated from the mother liquor by centrifugation. The precipitates were subsequently washed with twice-distilled water and with ethanol at the end, then dried under vacuum at room temperature (RT). Experimental conditions for the synthesis of samples are given in Table I.

pH values were measured using pH-meter (model pHM 26) manufactured by Radiometer. A combined pH electrode (pH range 0-14) was also manufactured by Radimeter. High pH values were measured by pH-paper with three colours (Merck).

^{57}Fe Mössbauer spectra were recorded in the transmission mode using standard instrumental configuration by WissEl GmbH (Starnberg, Germany). The ^{57}Co in the rhodium matrix was used as a Mössbauer source. The spectrometer was calibrated at 20 °C using the spectrum of a standard α-Fe foil. The velocity scale and all the data refer to the metallic α-Fe absorber at 20 °C. The experimentally observed Mössbauer spectra were fitted using the MossWinn program.

FT-IR spectra were recorded at RT using a Perkin-Elmer spectrometer model 2000. The FT-IR spectrometer was coupled to a personal computer loaded with the IRDM (IR data manager) program to process the recorded spectra. The specimens were pressed into small discs using a spectroscopically pure KBr matrix.

XRD patterns were recorded at 20 °C using an APD 2000 X-ray powder diffractometer (Cu Kα radiation, graphite monochromator, scintillation detector) manufactured by ItalStructures, Riva del Garda, Italy.

The thermal field emission scanning electron microscope (FE-SEM, model JSM-7000F), manufactured by Jeol Ltd. was linked to the EDS/INCA 350 (energy dispersive X-ray analyzer), manufactured by Oxford Instruments Ltd.

RESULTS AND DISCUSSION

Phase Analysis of Samples

Figure 1 shows the Mössbauer spectra of samples S1 to S8 at 20 °C, while the calculated Mössbauer parameters are given in Table II. The Mössbauer spectrum of sam-

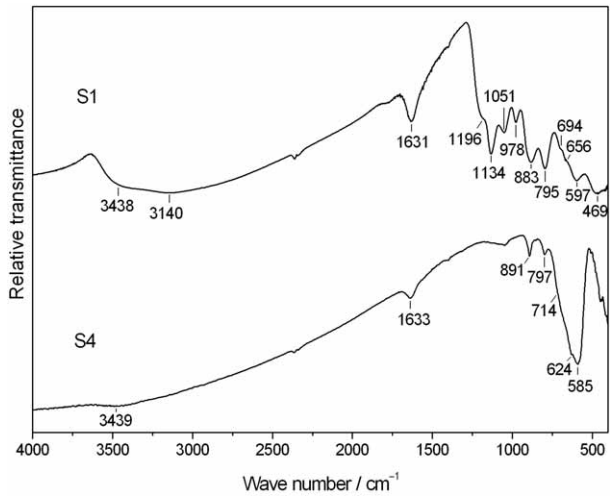

Figure 2. FT-IR spectra of samples S1 and S4, recorded at RT.

ple S1 is characterized by a central quadrupole doublet. Since the XRD analysis of sample S1 showed the presence of goethite as a single phase (Table I), it can be concluded that the spectrum of sample S1 corresponds to superparamagnetic goethite. Generally, the shape of the Mössbauer spectrum of goethite may vary from a well developed sextet having the intensity ratios 3:2:1:1:2:3 up to a paramagnetic doublet. The shape of the Mössbauer spectrum of goethite is influenced by the particle size, the degree of crystallinity and the content of »foreign« metal cations incorporated into the goethite crystal structure. Goethite particles smaller than 15–20 nm show a superparamagnetic type of the Mössbauer spectrum at RT, whereas the particles smaller than 8 nm show a superparamagnetic type of the Mössbauer spectrum down to 77 K.[10]

The presence of goethite in sample S1 was also confirmed by FT-IR spectroscopy, as shown in Figure 2. At high wave numbers a very broad and intensive IR band with shoulders at 3438 and 3140 cm^{-1} was recorded. The shoulder at 3438 cm^{-1} can be assigned to the stretching mode of H_2O molecules, whereas the shoulder at 3140 cm^{-1} can be assigned to the stretching mode of the OH group in a goethite structure. The IR band at 1631 cm^{-1} is due to the bending mode of H_2O molecules. Two bands at 883 and 795 cm^{-1} can be assigned to Fe-O-H bending vibrations in goethite. These two IR bands are typical of goethite, and they are usually used for the identification of this phase. The FT-IR spectrum of sample S1 also showed a shoulder at 1196 cm^{-1} and the bands at 1134, 1051 and 978 cm^{-1}. These IR bands can be assigned to sulphate groups, in line with an earlier work by Musić *et al.*[11] On the basis of the high intensity of these IR bands it can be inferred that sample S1 contained a significant amount of sulphate at external as well as internal surfaces (sulphated goethite).

The Mössbauer spectrum of sample S2 was fitted taking into account the superposition of the subspectra corresponding to goethite (0.59) and magnetite (0.41). In samples S3 and S4 the goethite fraction was significantly decreased (Table II), which is in line with XRD measurements (Table I). Magnetite is an inverse spinel and in its crystal structure one-third of iron as Fe^{3+} occupies all the available tetrahedral A-sites, one-third as Fe^{3+} occupies half of the octahedral B-sites, and one-third of Fe^{2+} occupies the other octahedral B-sites. The RT Mössbauer spectrum of Fe_3O_4 is characterized by two sextets corresponding to tetrahedral A-sites and octahedral B-sites. At low temperatures the Mössbauer spectrum of Fe_3O_4 is more complicated. Berry *et al.*[12] showed that the Mössbauer spectrum of Fe_3O_4 recorded at 4.2 K and in a zero external magnetic field was best fitted to five sextets. It was concluded that this Mössbauer spectrum reflected the Fe_3O_4 magnetic structure in which the Fe^{3+} tetrahedral A-site was ferrimagnetically coupled to two nonequivalent Fe^{3+} octahedral B-sites and two nonequivalent Fe^{2+} octahedral B-sites. In different precipitation processes the stoichiometry of magnetite usually deviates from an ideal formula Fe_3O_4. Magnetite comes as a substoichiometric $Fe_{3-x}O_4$, as also shown in the present work. The calculated stoichiometries of $Fe_{3-x}O_4$, based on our Mössbauer measurements, are given in Table II.

In the FT-IR spectrum of sample S4 (Figure 2) the relative intensities of IR bands at 891 and 797 cm^{-1}, corresponding to the goethite fraction, were significantly reduced. On the other hand, a very strong and broad IR band centered at 585 cm^{-1} appeared, and taking into account the result of the Mössbauer and XRD phase analy-

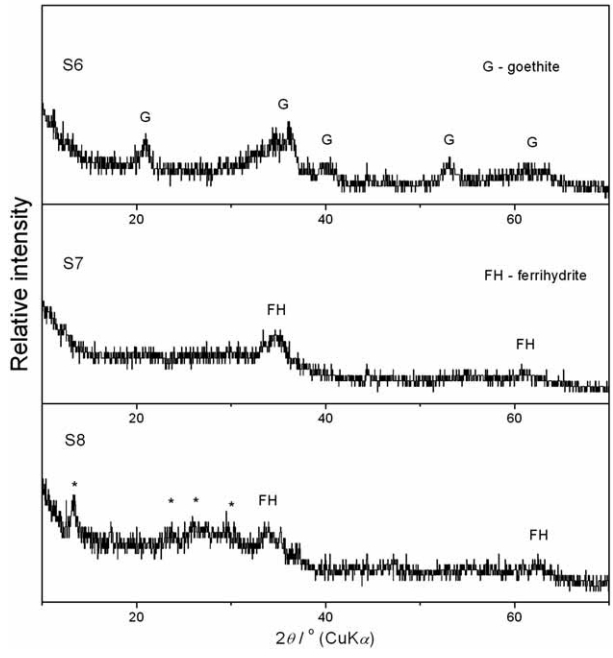

Figure 3. XRD patterns of samples S6 to S8, recorded at 20 °C.

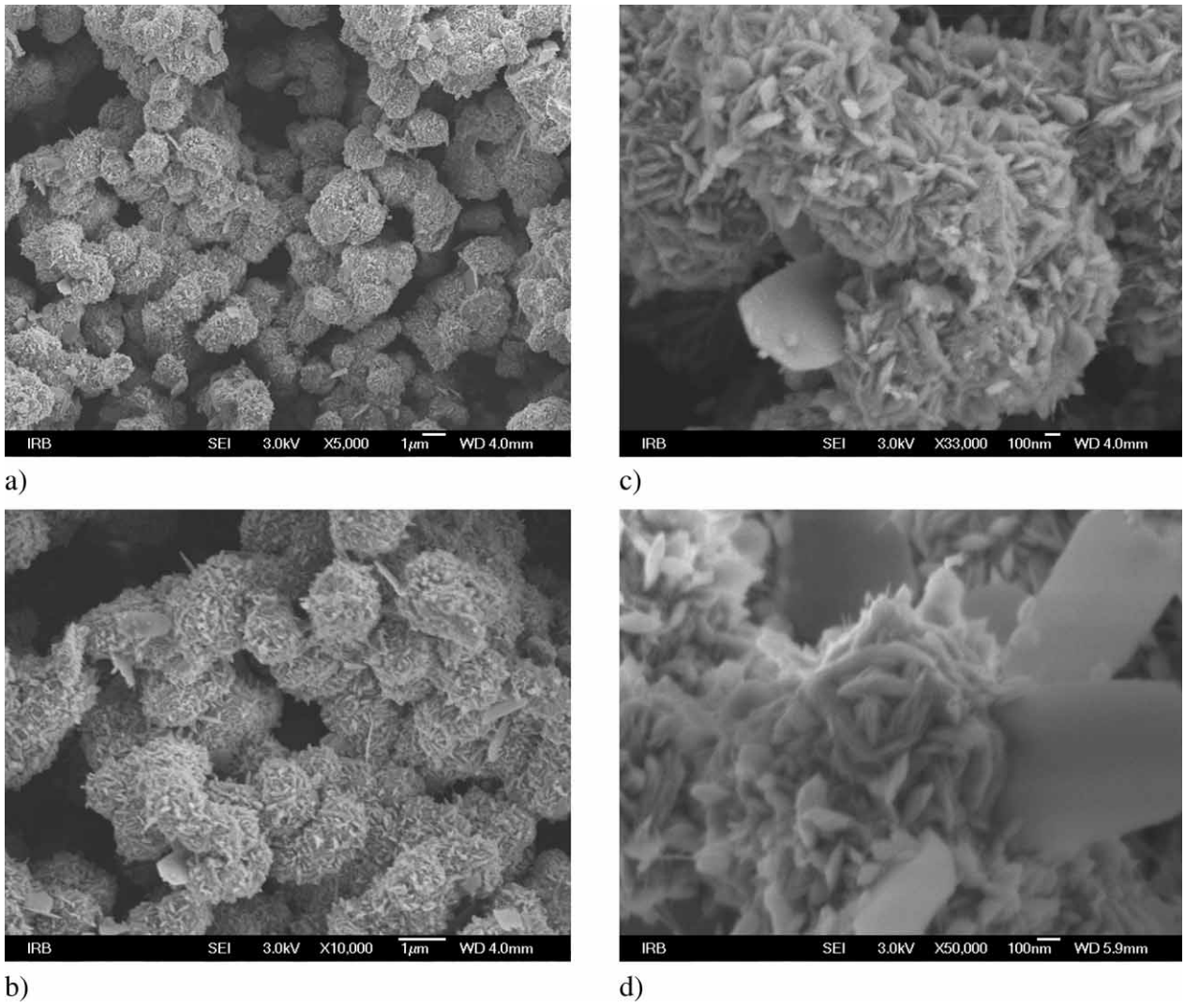

Figure 4. FE-SEM micrographs of sample S1 at different optical magnifications (a), (b), (c) and (d).

ses, this band can be assigned to magnetite. In an earlier work, Ellid *et al.*[13] recorded IR bands at 586 and 404 cm^{-1} for substoichiometric magnetite ($Fe_{2.91}O_4$). Ishii *et al.*[14] assigned the IR bands at 565 and 360 cm^{-1} to the ν_1 (F_{1u}) and ν_2 (F_{1u}) vibration modes in Fe_3O_4. The stoichiometry of magnetite influences the positions of these two IR bands.

The Mössbauer spectrum of sample S5 showed the presence of goethite and magnetite ($Fe_{3-x}O_4$). On the other hand, the spectra of samples S6, S7 and S8 showed only central quadrupole doublets at 20 °C. Taking into account the results of XRD measurement (Figure 3), the Mössbauer spectrum of sample S6 can be assigned to superparamagnetic goethite particles. The XRD pattern of sample S6 showed great broadening of goethite diffraction lines, thus indicating the presence of very fine particles.

XRD patterns of samples S7 and S8 (Figure 3) showed the presence of 2-line ferrihydrite. In sample S8 additional XRD lines (marked with an asterisk) are present, but they could not be assigned to a specific crystalline phase with any amount of certainty. The appearance of a central quadrupole doublet in the Mössbauer spectra of samples S7 and S8 at 20 °C is in accordance with the corresponding XRD phase analyses (Figure 3). Generally, the RT Mössbauer spectrum of ferrihydrite is fitted by researchers as a distribution of quadrupole splittings, a superposition of two doublets or simply as one average quadrupole doublet, as in the present case or the work by Žic *et al.*[15] Ristić *et al.*[16] have recently investigated the Mössbauer spectrum of poorly crystalline ferrihydrite down to 4.2 K, as well as in the presence of an external magnetic field.

FE-SEM and EDS

Figure 4 shows the FE-SEM micrographs of sample S1 at different optical magnifications and details. The phase analysis of this sample showed goethite as a single

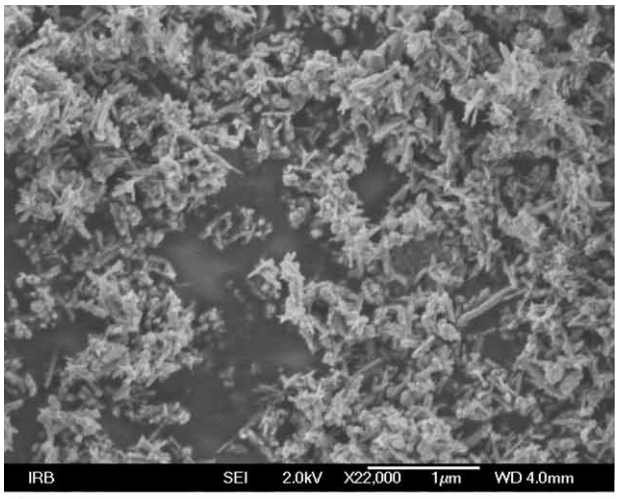

a)

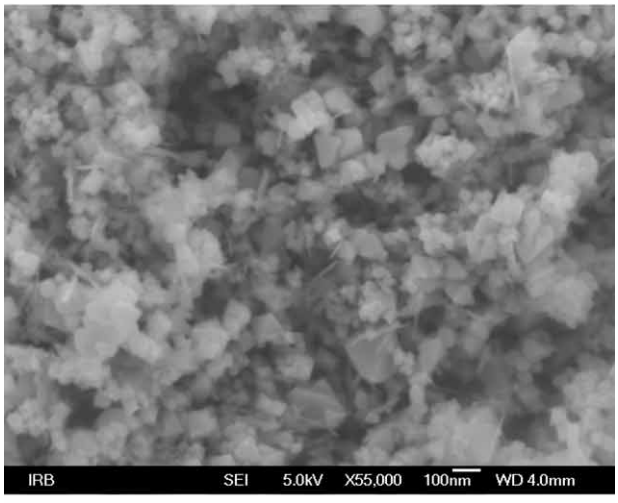

b)

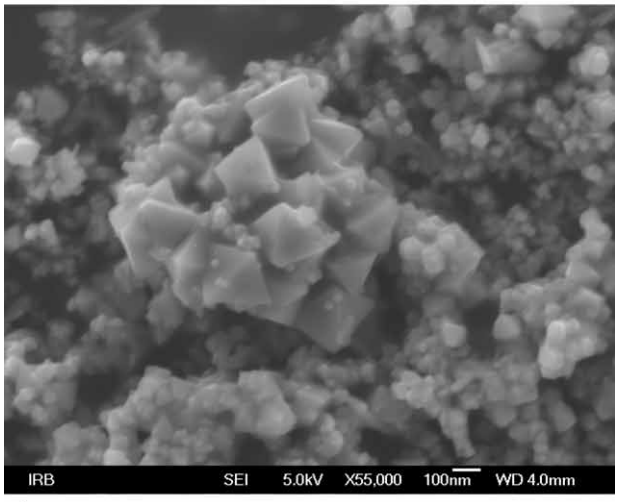

c)

Figure 5. FE-SEM micrographs of samples (a) S2, (b) S3 and (c) S4.

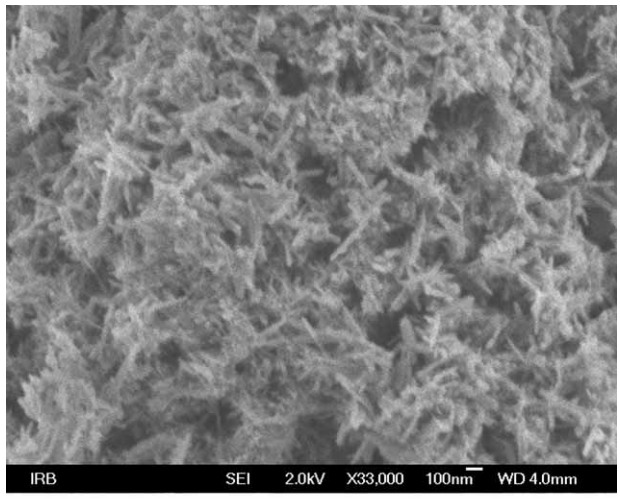

a)

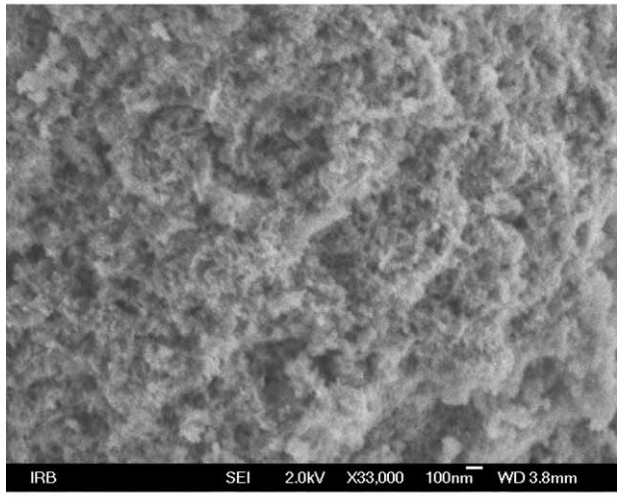

b)

Figure 6. FE-SEM micrographs of samples (a) S5, (b) S6.

phase, whereas the FT-IR spectrum of the same sample (Figure 2) also showed the presence of a significant amount of sulphate groups. At low optical magnification (Figures 4ab) near-spherical aggregates of goethite particles are well visible. Large plate-like goethite particles elongated along the crystallographic *c*-axis are also visible. More details are visible at higher optical magnification (Figures 4cd). In that sense, Figure 4d shows primary goethite particles in the form of small needles laterally arrayed, thus forming larger goethite particles close to a spindle shape. These goethite particles form near-spherical aggregates. This result shows that in the present case the formation of large goethite particles is governed by the aggregation mechanism. Figure 4d also shows large elongated plate-like goethite particles formed in parallel. Figure 5 shows the FE-SEM micrographs of samples S2, S3 and S4. It is evident that the addition of TMAH and a corresponding increase in the pH resulted in strong changes in the aggregation of goethite particles (Figure 5a). Goethite particles combined a rod-like shape with varying sizes; some of them have grown ≈750 nm long. The width of primary goethite particles was ≈15 nm.

Primary particles also showed a tendency toward lateral aggregation as in the previous case; however, in sample S2 they aggregated producing larger rods. In some cases the formation of dendritic particles was also observed. Figure 5b shows that the formation of magnetite particles is dominant, which is in line with the phase analysis. Two kinds of magnetite particles were observed: (a) aggregates of magnetite particles varying in size from ≈20 to ≈100 nm, and (b) separate magnetite particles up to ≈200 nm in size. In sample S4 (Figure 5c) the aggregation of smaller magnetite particles is more pronounced than in sample S3, whereas well-defined octahedral magnetite particles also showed a tendency toward aggregation as well as twin formation. In samples S3 and S4 the fractions of rod-like goethite particles were significantly decreased, which is also in line with the results of phase analysis.

Figure 6 shows the FE-SEM micrographs of samples S5 and S6. In these samples goethite particles are rod-like. In sample S5 some goethite rods reached 500 nm in length, whereas in sample S6 very small goethite rods ≈15–25 nm were obtained. Figure 7 shows the FE-SEM micrographs of samples S7 (Figures 7ab) and S8 (Figures 7cd) at different optical magnifications. Very small pseudospherical particles and amorphous-like aggregates were observed. During the long-time exposition of samples (not coated) in a high vacuum electron microscope chamber we have observed the loss of water and the appearance of rod-like particles as the result.

Figure 8 shows the EDS spectra of selected samples S5 and S8. The sulphur concentration did not change significantly in samples S5 to S8; the phosphorus concentration, however, increased significantly from sample S5 to S8. Geelhoed *et al.*[17] investigated adsorption of phosphate or sulphate as a single adsorbate, as well as the mixture of phosphate and sulphate adsorbates on goethite surfaces. The concentration of phosphate varied from 10^{-8} to 10^{-4} mol dm^{-3} and of sulphate varied from 10^{-5} to 10^{-3} mol dm^{-3}. In competitive adsorption systems containing both phosphate and sulphate adsorbates, phosphate was

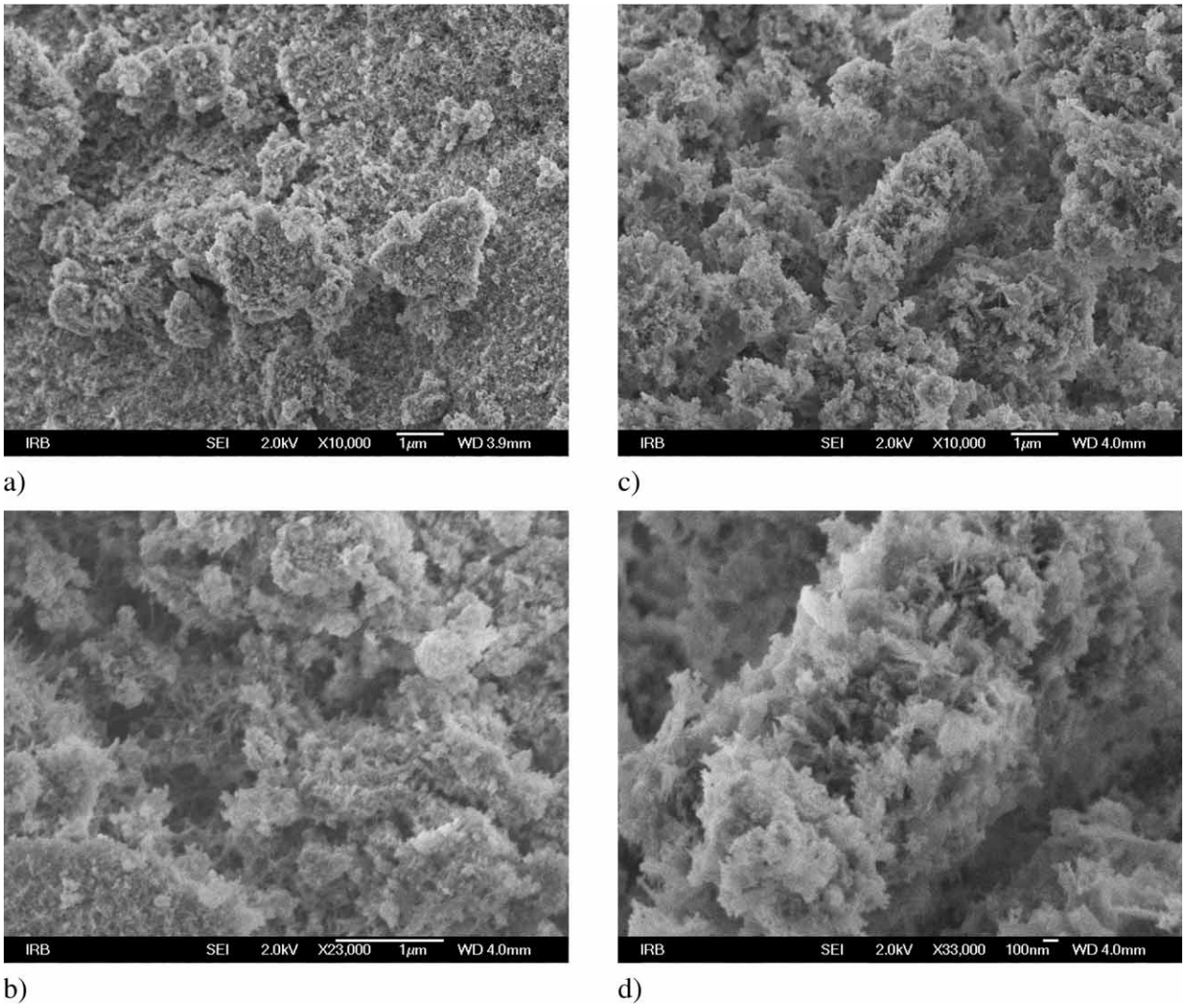

Figure 7. FE-SEM micrographs of samples (a, b) S7 and (c, d) S8 at different optical magnifications.

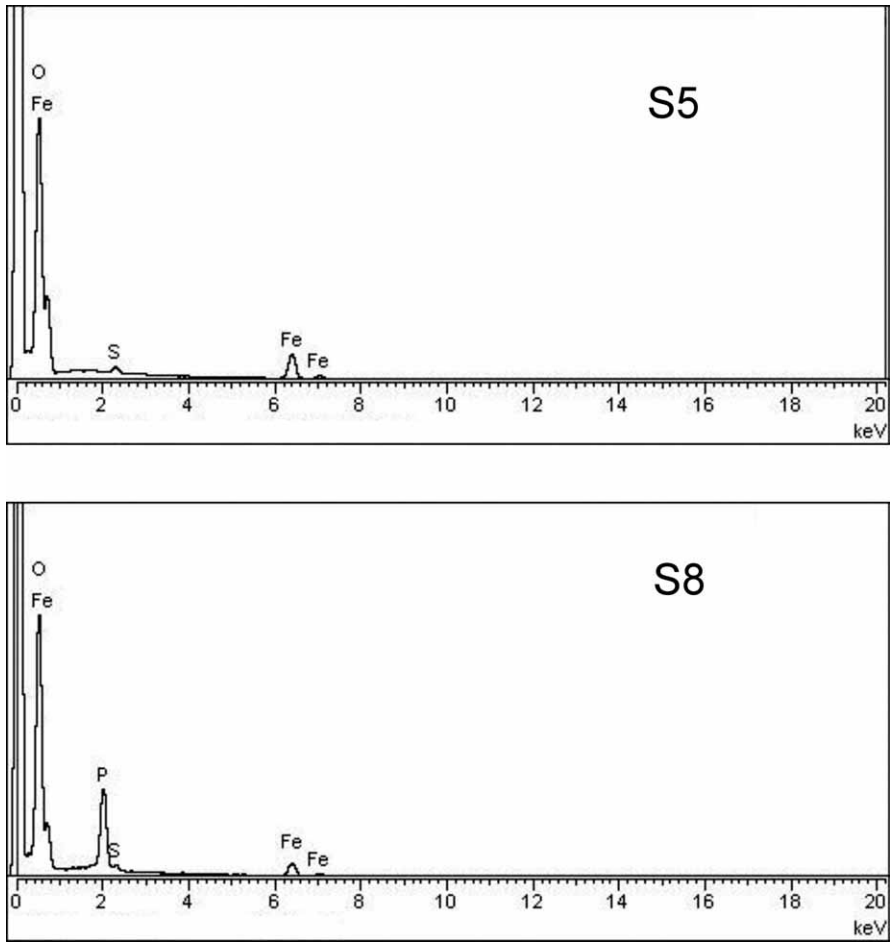

Figure 8. EDS spectra of selected samples S5 and S8.

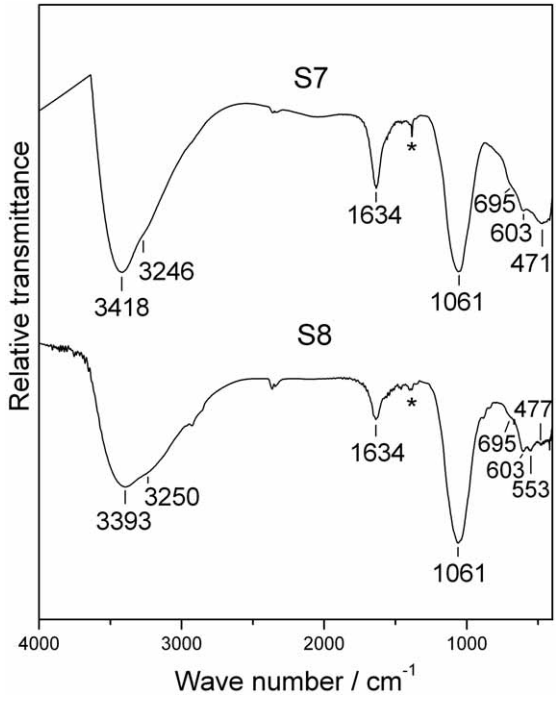

Figure 9. FT-IR spectra of samples S7 and S8, recorded at RT. (*) – parasitic line.

a stronger competitor for adsorption sites on goethite than sulphate. This is consistent with a higher affinity of phosphate for goethite surfaces compared with sulphate. However, the presence of sulphate caused a small decrease in phosphate adsorption per unit surface area on goethite at a relatively low pH.

In the present work, at mild acidic conditions the formation of goethite was strongly suppressed by an increased phosphate concentration. Poor crystalline ferrihydrite (two-line) was formed instead. At a low concentration of phosphate, as well as sulphate, there is specific adsorption of these anions. The preferential nature of this adsorption process may strongly influence the shape of the particles. For example, goethite particles can be strongly elongated along the crystallographic *c*-axis. At a high concentration of phosphate or sulphate there is precipitation of these anions on (hydrous)oxide adsorbent. Ler and Stanforth[18] proposed a model for surface precipitation of phosphate on goethite. In accordance with this model there is a dissolution of Fe^{3+} ions, which in the next step react with the already present phosphate group at the surface of goethite particles, then the cycle can be repeated with the adsorption of phosphate, *etc*.

Phosphated ferrihydrite (samples S7 and S8) showed a very strong and broad IR band at 1061 cm^{-1} (Figure 9). The separation of IR bands corresponding to phosphate[19–21] or sulphate[11] groups is not visible. The IR band at 1061 cm^{-1} recorded for phosphated ferrihydrite due to its complexity could not be attributed with certainty to specific vibrations.

CONCLUSION

- Needle-like goethite particles were obtained by a simple oxidation of the $FeSO_4$ solution (suspension) with pure oxygen at 90 °C. Primary particles showed a tendency toward lateral arraying and building of larger particles close to the spindle-shape. Secondary particles formed in the next step were the near-spherical aggregates of goethite. Wide and thin goethite particles, which were markedly elongated along the *c*-crystallographic axis, were formed in parallel.
- With the addition of TMAH and a corresponding pH-increase, the magnetite phase was additionally formed. At pH ≈ 12.5 and higher, a mixture of magnetite and several % of goethite was obtained. In all samples containing magnetite the substoichiometry of this phase was observed by Mössbauer spectroscopy and the corresponding stoichiometries of $Fe_{3-x}O_4$ were determined.
- Magnetite particles (≈ 20–100 nm) showed a tendency toward aggregation. For larger octahedral magnetite particles (> 200 nm) aggregation and the twinning effect were also observed. Adding orthophosphoric acid to the precipitation system containing 0.01 mol dm^{-3} $FeSO_4$ + 0.01 mol dm^{-3} H_2SO_4 at the start had a drastic effect on the properties of the precipitate. In the presence of 5×10^{-3} mol dm^{-3} H_3PO_4 nanosize goethite particles (≈15–25 nm) were obtained. In the presence of 1.25×10^{-2} mol dm^{-3} and 2.5×10^{-2} mol dm^{-3} H_3PO_4 two-line ferrihydrite was found by XRD. The EDS analysis showed that the sulphur content did not change significantly in the precipitates. On the other hand, the phosphor content in precipitate gradually increased from sample S5 to S8. The FT-IR spectrum of phosphated ferrihydrite showed a very strong and broad IR band centered at 1061 cm^{-1}. In samples S7 and S8 phosphate anions suppressed the formation of goethite, so phosphated ferrihydrite was formed instead.

REFERENCES

1. R. M. Cornell and U. Schwertmann, *The iron oxides: structure, properties, reactions, occurrence and uses*, VCH Publ., 1996, D-69451 Weinheim, Germany.
2. S. Musić, I. Czakó-Nagy, S. Popović, A. Vértes, and M. Tonković, *Croat. Chem. Acta* **59** (1986) 833–851.
3. S. Musić, S. Popović, and M. Gotić, *Croat. Chem. Acta* **60** (1987) 661–675.
4. S. Musić, S. Popović, and M. Gotić, *J. Mater. Sci.* **25** (1990) 3186–3190.
5. M. Gotić and S. Musić, *J. Mol. Struct.* **834–836** (2007) 445–453.
6. E. Matijević, R. S. Sapieszko, and J. B. Melville, *J. Colloid Interface Sci.* **50** (1975) 567–581.
7. R. S. Sapieszko, R. C. Patel, and E. Matijević, *J. Phys. Chem.* **81** (1977) 1061–1068.
8. S. Musić, A. Vértes, G. W. Simmons, I. Czakó-Nagy, and H. Leidheiser Jr., *J. Colloid Interface Sci.* **85** (1982) 256–266.
9. S. Musić, Z. Orehovec, S. Popović, and I. Czakó-Nagy, *J. Mater. Sci.* **29** (1994) 1991–1998.
10. E. Murad and J. H. Johnston, *Iron Oxides and Oxyhydroxides in Mössbauer Spectroscopy Applied to Inorganic Chemistry*, in: G. J. Long (Ed.), Vol. 2, Plenum Publishing Corporation, 1987, pp. 507–582.
11. S. Musić, A. Šarić, S. Popović, K. Nomura, and T. Sawada, *Croat. Chem. Acta.* **73** (2000) 541–567.
12. F. J. Berry, S. Skinner, and M. F. Thomas, *J. Phys.: Condens. Matter* **10** (1998) 215–220.
13. M. S. Ellid, Y. S. Murayed, M. S. Zoto, S. Musić, and S. Popović, *J. Radioanal. Nucl. Chem.* **258** (2003) 299–305.
14. M. Ishii, M. Nakahira, and T. Yamanaka, *Solid State Commun.* **11** (1972) 209–213.
15. M. Žic, M. Ristić, and S. Musić, *J. Mol. Struct.* **834–836** (2007) 141–149.
16. M. Ristić, E. De Grave, S. Musić, S. Popović, and Z. Orehovec, *J. Mol. Struct.* **834–836** (2007) 454–460.
17. J. S. Geelhoed, T. Hiemstra, and W. H. van Riemsdijk, *Geochim. Cosmochim. Acta* **61** (1997) 2389–2396.
18. A. Ler and R. Stanforth, *Environ. Sci. Technol.* **37** (2003) 2694–2700.
19. M. Nanzyo and Y. Watanabe, *Soil Sci. Plant Nutr.* **28** (1982) 359–368.
20. P. Persson, N. Nilsson, and S. Sjöberg, *J. Colloid Interface Sci.* **177** (1996) 263–275.
21. E. J. Elzinga and D. L. Sparks, *J. Colloid Interface Sci.* **308** (2007) 53–70.

SAŽETAK

Istraživanje faktora koji utječu na taloženje željezovih oksida iz otopina Fe(II)

Marijan Gotić, Svetozar Musić, Stanko Popović i Lavoslav Sekovanić

Istraživani su faktori koji utječu na taloženje željezovih oksida iz otopina Fe(II) primjenom difrakcije X-zraka u prahu, ^{57}Fe Mössbauerovom i FT-IR spektroskopijama te FE-SEM i EDS tehnikama. Oksidacijom 0,1 mol dm^{-3} otopine (suspenzije) $FeSO_4$ sa čistim kisikom pri 90 °C dobiveni su približno sferni agregati vretenastih čestica getita. Široke i tanke čestice getita izdužene u smjeru kristalogrfske *c*-osi nastale su u isto vrijeme. Podstehiometrijske čestice magnetita ($Fe_{3-x}O_4$) dodatno su nastale, nakon što je tetrametilamonijev hidroksid dodan u otopinu (suspenziju) 0,1 mol dm^{-3} $FeSO_4$. Te čestice bile su dominantne pri pH > 12,5. Mössbauerova spektroskopija je primijenjena pri određivanju stehiometrije čestica $Fe_{3-x}O_4$. Vrlo male čestice magnetita (≈20–100 nm) pokazale su tendenciju stvaranja agregata. Oktaedarske čestice magnetita veće od 200 nm pokazale su tendenciju stvaranja kristala sraslaca. Jak efekt na svojstva taloga željezovih oksida postignut je dodavanjem H_3PO_4 u taložni sustav koji je sadržavao otopinu 0,1 mol dm^{-3} $FeSO_4$ + 0,1 mol dm^{-3} H_2SO_4 na samom početku taloženja. Nanočestice getita veličine 15–25 nm ili slabo kristalne čestice ferihidrita (dvolinijski ferihidrit) ovisile su o koncentraciji dodane kiseline H_3PO_4. EDS analize taloga nisu pokazale značajne promjene sadržaja sumpora, dok se sadržaj fosfora stupnjevito povećavao u talozima s povećanjem koncentracije dodane kiseline H_3PO_4. Pri visokim koncentracijama iona fosfata nastajanje getita moglo je biti u potpunosti potisnuto, a umjesto getita došlo je do nastajanja fosfatiziranog ferihidrita.